

Supplementary Figures

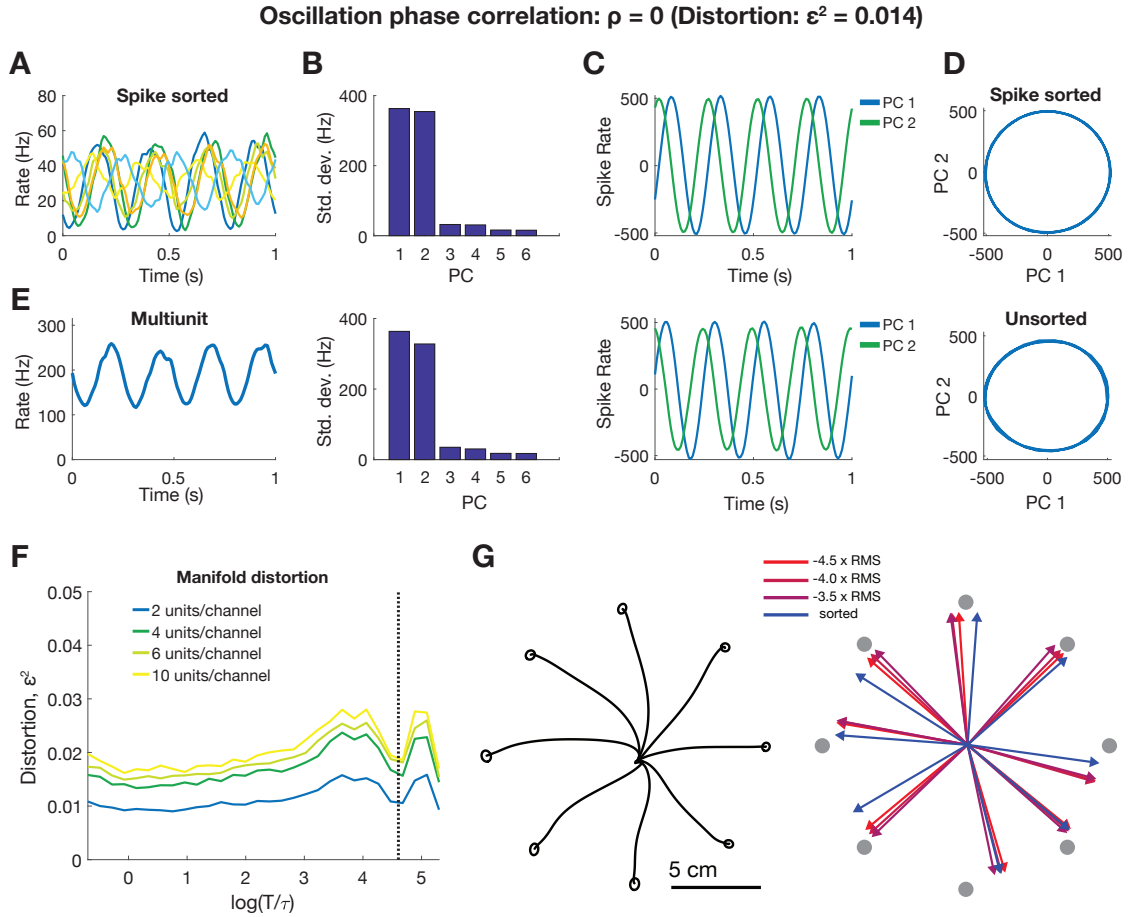


Figure S1: Related to Figure 2: **Simulation of the effect of spike sorting on oscillations.** We simulate the response of oscillating neurons, with independently generated random phases, through 200 channels. Each neuron spikes with a Poisson distribution with a mean rate of 40 Hz when averaged over the period of oscillation. Simulated spikes are smoothed with a $\sigma = 10$ ms width Gaussian filter and averaged over 100 trials to produce PSTHs. **(A)** An example of PSTHs from oscillating units with period $\tau = 0.1$ s contributing to one of the channels (first row) and the effective PSTH of the channel (second row), i.e., the sum of all the individual neurons' firing. From left to right, we show the example neuron/channel's PSTHs, the standard deviations of each principal component of the 200 channel population activity, the principal components themselves, and the firing rate manifolds projected onto the first two principal components. The PCA spectrum is dominated by the first two components: the sine and cosine modes, roughly tracing out a circle in firing rate space. **(B)** Distortion of firing rate manifold resulting from combining units with oscillation period τ varying from 5 ms (i.e. shorter than the smoothing window) to 2 s (i.e. longer than the simulation duration). The distortion is very small with little dependence on the oscillation period, except for a blip when $\tau \leq \sigma$ indicated by the vertical dotted line. **(G)** (left) Hand trajectories and reach endpoint covariance ellipsoids for dataset N20101105. (Right) Population vector decode of reach direction using binned spike counts during the peri-movement period from sorted and threshold crossings at multiple threshold levels for this dataset.

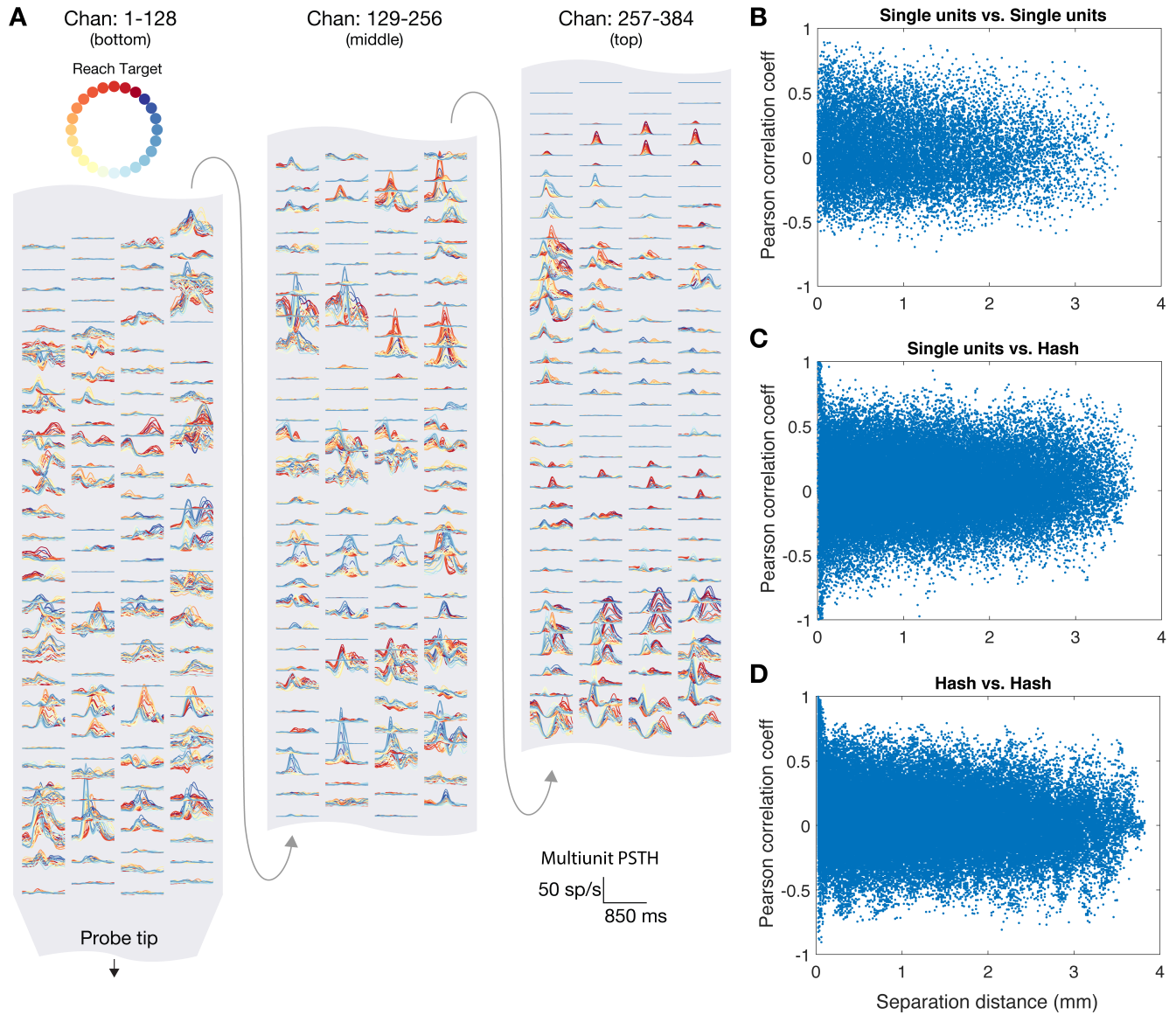


Figure S2: Related to Figure 3: **Dense recordings reveal a lack of localized tuning properties in primate PMd** (A) multi-unit PSTHs recorded using Neuropixels probe. Each inset panel represents 24 multi-unit PSTHs, colored by reach direction, mapped to spatial location on the probe. Adjacent electrode sites frequently share similar tuning properties due to single neurons appearing on multiple electrodes. (B) Scatterplot of pairwise correlation of neuron PSTHs as a function of separation distance between neurons. (C) Pairwise correlations between single units and multi-unit "hash" PSTHs. (D) Pairwise correlations between multi-unit "hash" PSTHs on different electrodes. The clustered correlations (mass of points in the top left) is the result of single neurons appearing on multiple channels. Spike sorting eliminates this relationship between distance and correlation in tuning, shown in the top plot.

Isolated Neurons

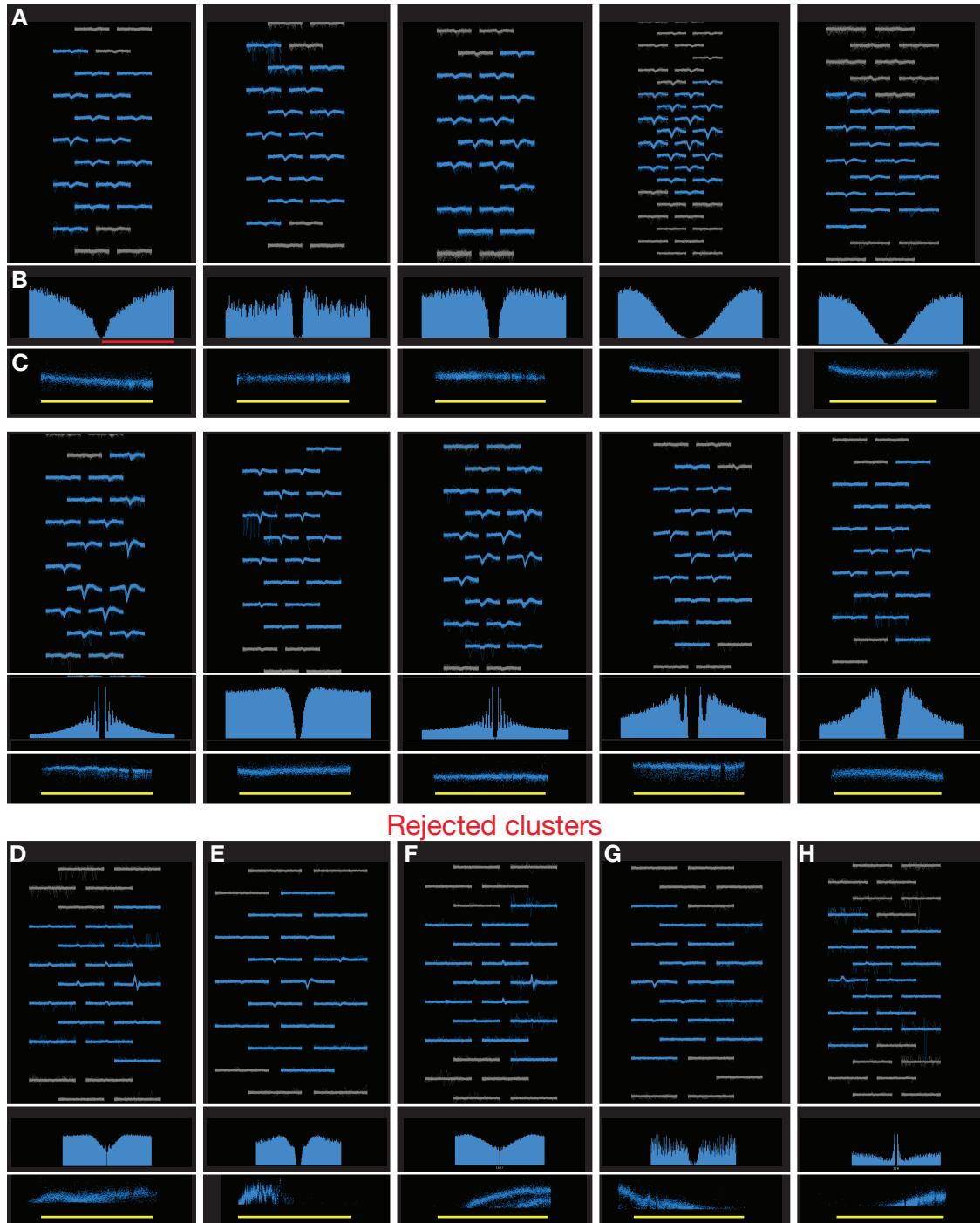


Figure S3: Related to Figure 3: **Example spike sorting results using Neuropixels probe data.** (A) Waveform snippets corresponding to spikes from a single neuron, mapped to spatial location along the probe. Adjacent contacts are approximately 20 micrometers apart. (B) Autocorrelogram for spikes corresponding to this neuron's cluster after sorting. Bin width is 0.5 ms, red bar represents 100 ms (same format for all panels). (C) Waveform template amplitude (arbitrary units) throughout the duration of the recording session showing stable isolation for the full duration of the experiment (yellow bar: approximately 2 hours). Slight changes in template amplitude are normal due to micro-scale tissue motion, and not problematic as long as a unit can be tracked for the full recording duration. (D) Example rejected multi-unit cluster (frequent inter-spike interval violations in autocorrelogram). (E) Example rejected unstable unit (bottom panel - no spike present after the start of the recording (F-H) Other examples of rejected clusters due to multi-unit or not stable for the full recording duration.

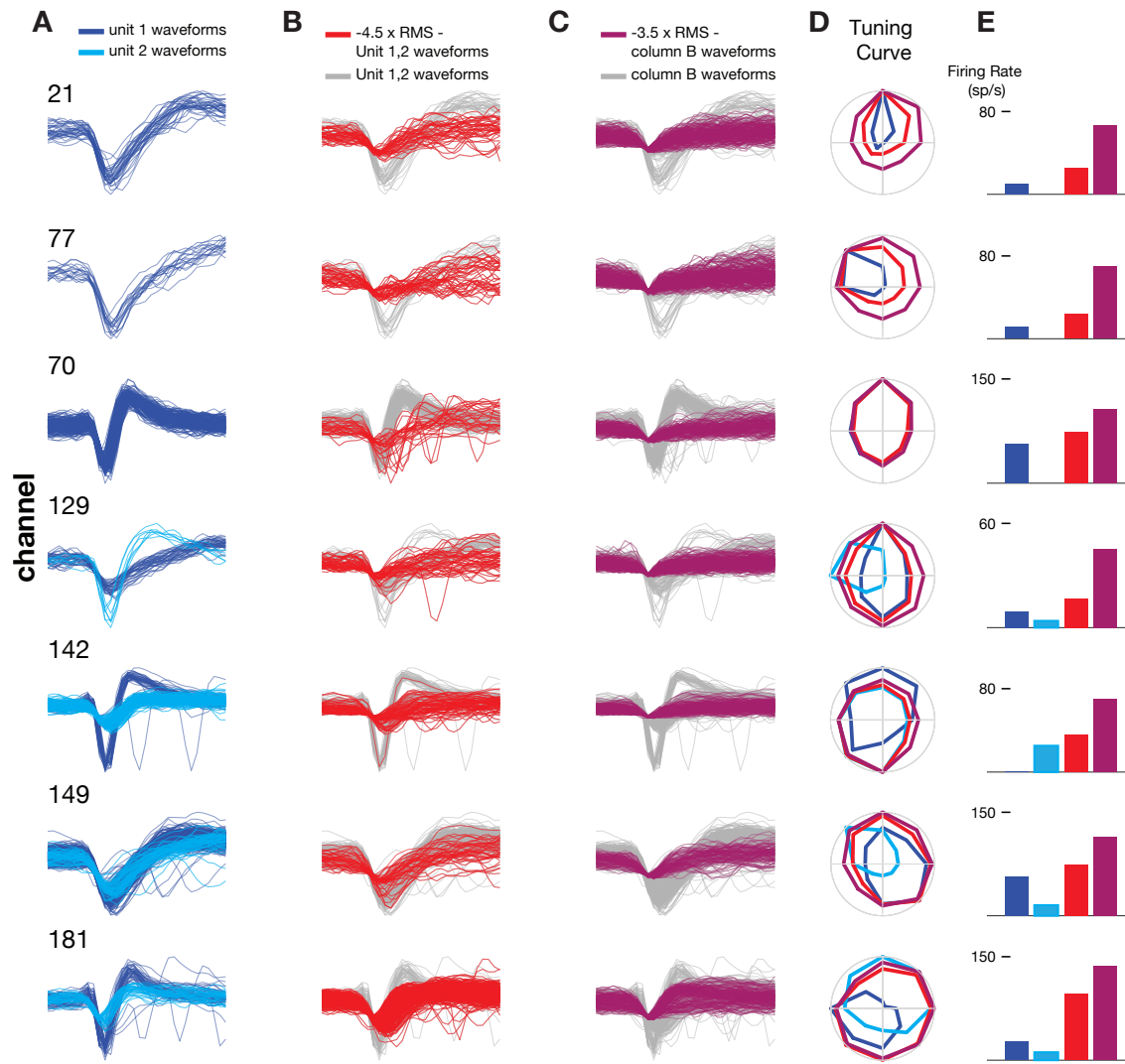


Figure S4: Related to figure 4: **Waveforms and tuning of single units and threshold crossings** (A) Hand-isolated waveforms from channels with either one or two units. (B) All waveforms detected using signal threshold $-4.5 \times$ RMS. Additional waveforms not already present in (A) are highlighted in red. (C) All waveforms detected using signal threshold $-3.5 \times$ RMS. Additional waveforms added not already present in (B) or (A) are shown in purple. (D) Firing rate tuning curves during reaches to eight radially spaced targets for the three thresholding levels shown in A-C. Consistent with expectations, more permissive thresholds broaden tuning curves but generally preserve peak tuning direction. (E) Firing rate for peak tuning direction for each threshold level A-C. More permissive thresholds result in higher firing rates.

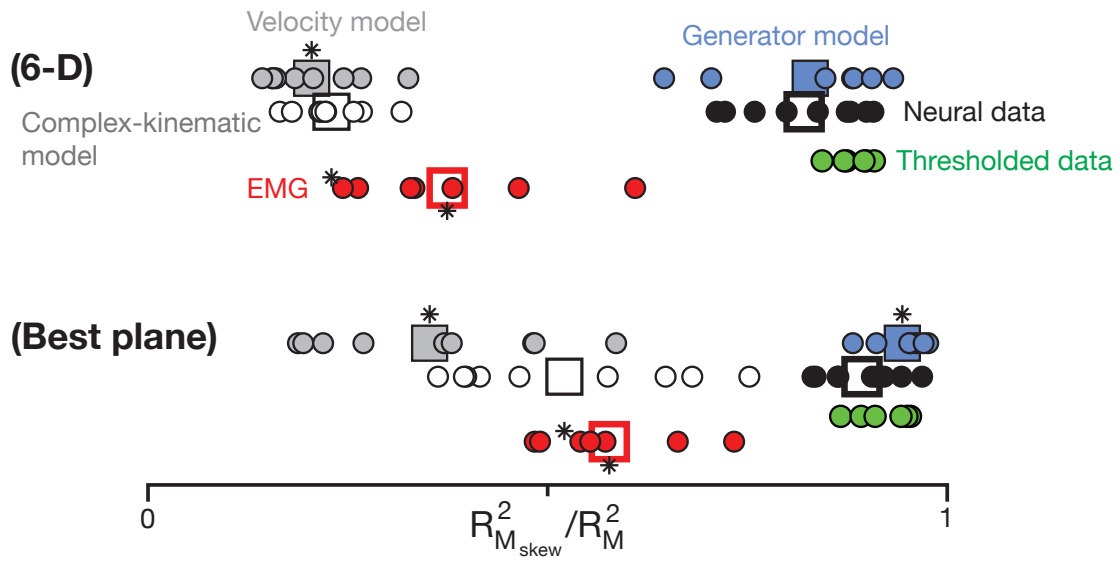


Figure S5: Related to Figure 5: **Consistency of rotational dynamics of thresholded data** Figure reproduced from (Churchland et al. 2012, Figure 6), with additional data points for the re-thresholded data sets (green), illustrating that the ratio $R^2_{M_{skew}} / R^2_M$ for thresholded datasets is consistent with hand sorted neural data.

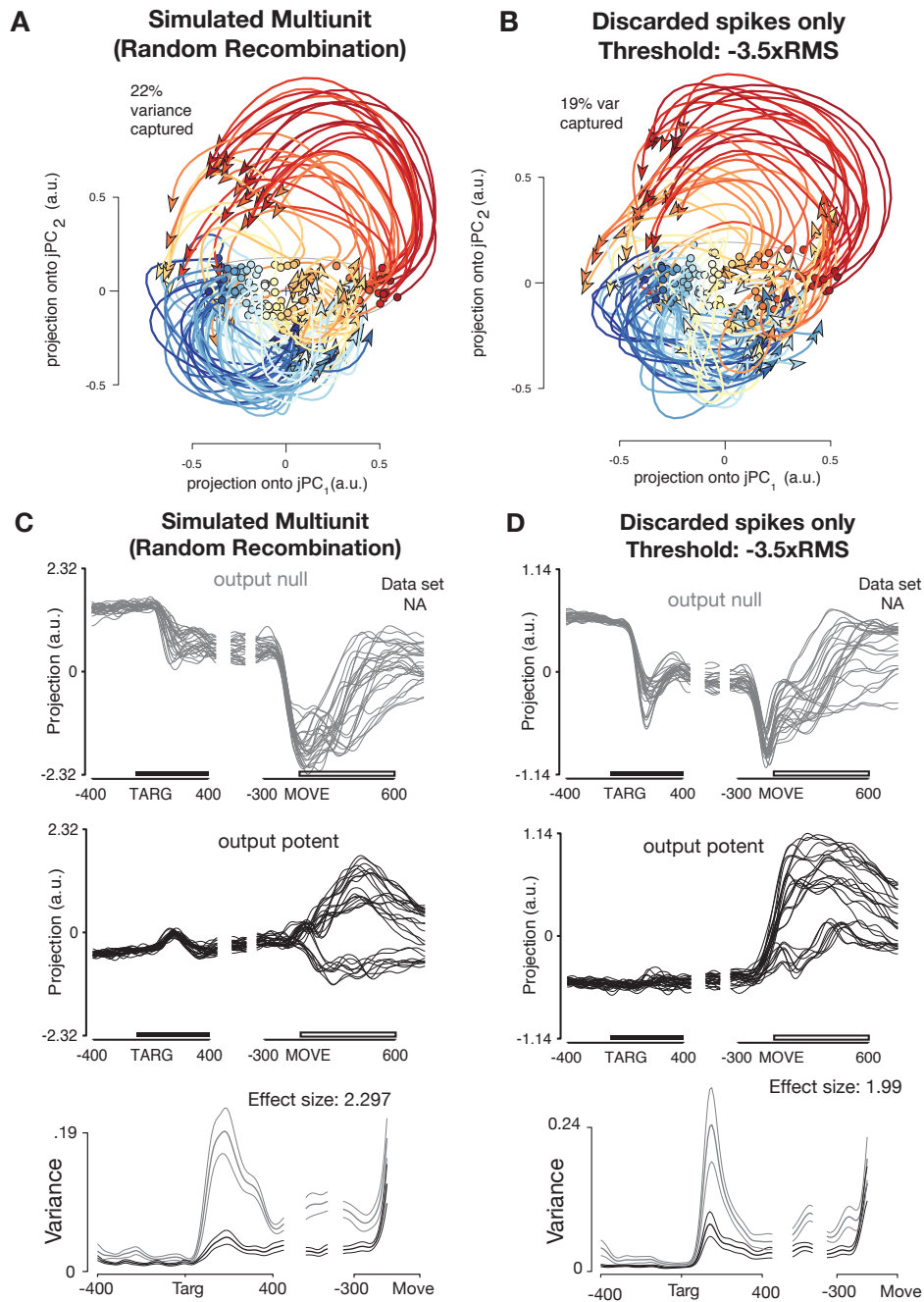


Figure S6: Related to Figures 5 and 6: **Study replication using simulated multiunit and discarded threshold crossings.** Both studies using both analysis types support the conclusions and findings of the original studies, respectively. **(A)** Churchland et al. 2012 results using isolated single units which were randomly recombined to create simulated multiunit activity. **(B)** Churchland et al. 2012 replication using only threshold crossings discarded during spike sorting. **(C)** Kaufman et al. 2014 replication using simulated multiunit **(D)** Kaufman et al. 2014 replication using only discarded threshold crossings.

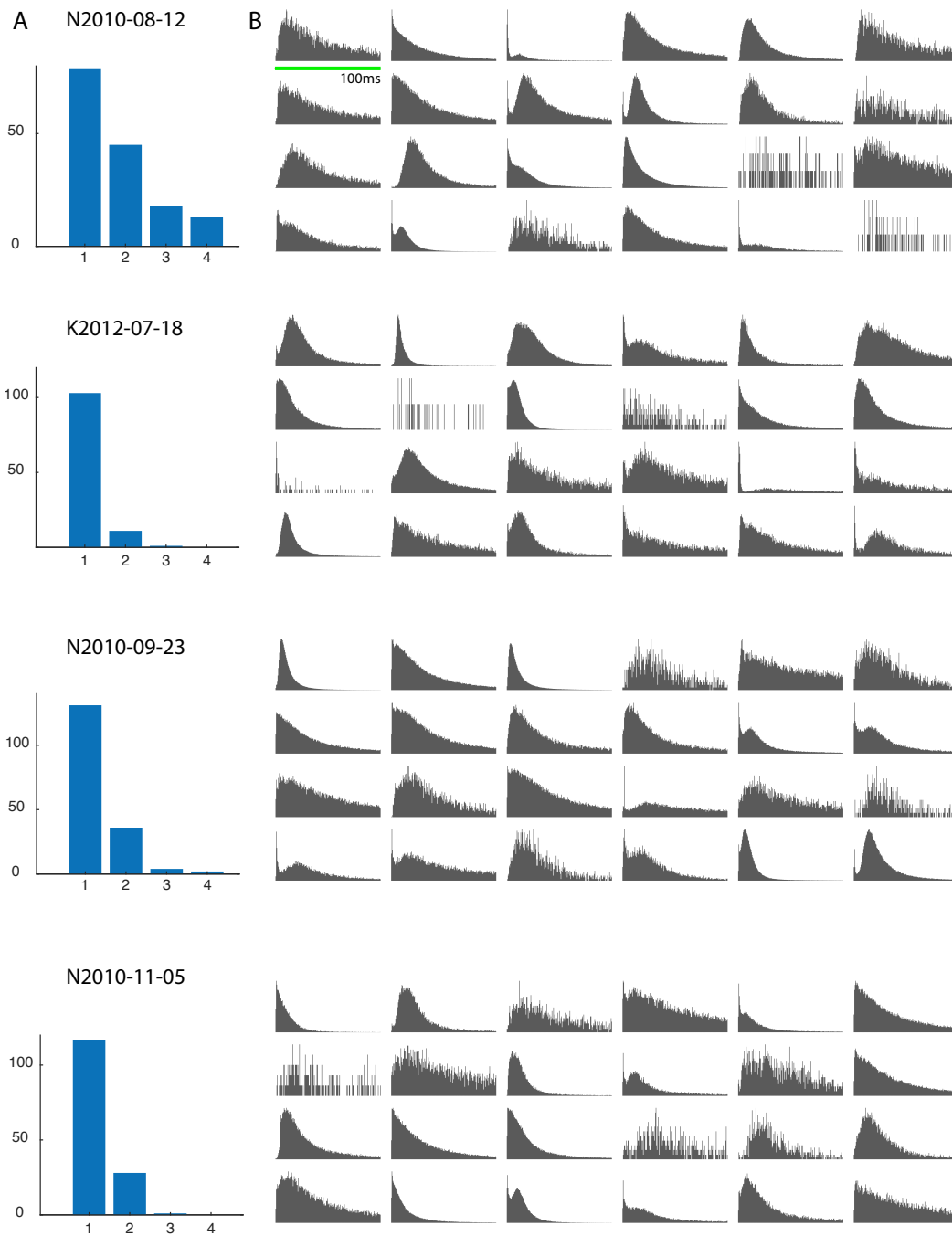


Figure S7: Related to Figures 4-6: **Utah array dataset unit isolation information** (A) Histograms of number of isolated units per recording channel for four datasets collected using Utah arrays. (B) Inter-spike interval distributions for 24 randomly selected neurons for each dataset presented in (A). Green bar: 100ms.